Adsorption of Dibenzothiophene on Ag/Cu/Fe-Supported Activated Carbons Prepared by Ultrasonic-Assisted Impregnation

Jing Xiao, Guoan Bian, Wei Zhang, and Zhong Li*

Research Institute of Chemical Engineering, South China University of Technology, Guangzhou 510640, People's Republic of China

This work is mainly involved with study of the adsorption of dibenzothiophene (DBT) on Ag/Cu/Fe-supported activated carbons (ACs) prepared by ultrasound-assisted impregnation (UI). Ag/AC-UI, Cu/AC-UI, and Fe/AC-UI were separately prepared by using impregnation of different metal salt solutions under ultrasound irradiation (UIr) and characterized by X-ray photoelectron spectroscopy (XPS) and CO-chemisorption experiments. Isotherms of DBT on the modified ACs were separately measured, and the effects of different metal ions loaded on the ACs on the amount of adsorbed DBT on the modified ACs are discussed. Results indicated that (1) the DBT adsorption capacity of the ACs modified by using impregnation without UIr followed the order: Ag/AC > Cu/AC > AC > Fe/AC; (2) the modification methods have significant influence on the adsorption abilities of the modified ACs toward DBT. The application of UIr to prepare metal ion-impregnated ACs can make the metallic particles on the carbon surfaces become finer and disperse better in comparison with the use of impregnation only. As a consequence, the Ag/AC-UI and Cu/AC-UI prepared by using the UIr have higher adsorption capacities of DBT than the Ag/AC and Cu/AC prepared using impregnation.

1. Introduction

Sulfur compounds in fuels are converted to SO_x during combustion, which not only results in acid rain but also poisons catalysts in catalytic converters for reducing CO and NO_x.[1] Primarily for environmental concerns, governments worldwide have issued increasingly stringent regulations to limit sulfur levels in fuels. The United States Environmental Protection Agency (EPA) has mandated the maximum sulfur content from the current level of (300 to 500) ppm by weight (ppmw) to 10 ppmw in gasoline and diesel in 2010.[2] The European Union has issued regulations to reduce the sulfur content of gasoline from a current average of (150 to < 10) ppmw in 2009.[3] Therefore, the petroleum refining industry is facing a major challenge to produce the ultraclean liquid hydrocarbon fuels to meet stricter sulfur specifications, and ultra-deep desulfurization of liquid hydrocarbon fuels has received increasing attention.

Currently, the major desulfurization technology is hydrodesulfurization (HDS), which is carried out at elevated temperatures and hydrogen partial pressures to convert organosulfur compounds to hydrogen sulfide (H_2S).[4] The HDS process is highly efficient in removing thiols and sulfides, but not for thiophenes and thiophene derivatives. Thus, after the conventional HDS processes, the major sulfur compounds remaining in the transportation fuels are the refractory sulfur compounds, mainly dibenzothiophene (DBT) and its alkylated derivatives.[5] The removal of these molecules selectively is mandatory to meet the new environmental specifications.

One of the major methods for selective desulfurization from fuels is adsorption by using porous solid adsorbents. Since activated carbon (AC) is one of the most important adsorbents dominating the commercial use of adsorption due to its porous structure with high surface area and large pore volume, it has widely been studied for the adsorptive removal of pollutants from both gas and liquid phases.[6–10] To further develop highly efficient desulfurization adsorbents for ultraclean fuels, modification of AC[1,11–15] has received considerable attention. Among them, transitional metal ion-loaded ACs show great application potential.[11,12] Wang and Yang used $CuCl/AC$, $PdCl_2/AC$, and Pd/AC for the desulfurization of a model jet fuel by selective adsorption of thiophenic molecules and reported that the sulfur adsorption capacity of $PdCl_2/AC$ was higher than that of $CuCl/AC$ and Pd^0/AC, in agreement with molecular orbital results.[11] Ania and Bandosz used metal-loaded carbon-based sorbents containing sodium, cobalt, copper, and silver as DBT removal media via reactive adsorption. The metals incorporated to the surface act not only as active sites for selective adsorption of sulfur-containing aromatic compounds but also as structural stabilizers of the carbon materials and as catalyst initiators in reactive adsorption. It was also reported that cobalt and copper loaded carbons showed the highest uptake, due to not-well-defined catalytic synergistic effects.[12] Zhou et al. examined the effects of structural and surface properties of carbon materials on adsorption desulfurization, and reported that different carbon materials have significantly different sulfur-adsorption capacities and selectivities that depend not only on textural structure but also on surface functional groups.[13] Recently, Zhou et al. reported that HNO_3 oxidation of AC was an effective method in improving adsorption performance of sulfur compounds, due to an increase in the acidic oxygen-containing functional groups, suggesting that the adsorption of sulfur compounds over the AC may involve an interaction of the acidic oxygen-containing groups on AC with the sulfur compounds.[14] Yu et al. applied thermal oxidation on AC for the adsorption of DBT; their results indicated that the higher the oxidation temperature was, the larger were the amounts of surface acidic oxygen-containing groups, and thus the higher were the amounts of DBT adsorbed on corresponding carbons.[15]

Recently, the use of ultrasound irradiation (UIr) has been investigated as a means to initiate or induce chemical modifica-

* Corresponding author. Fax: +86-20-87110608. E-mail address: cezhli@scut.edu.cn.

tion on many materials.[16] Effects induced by ultrasound in aqueous solution have been attributed to acoustic cavitation, that is, the formation, growth, and collapse of bubbles in a liquid.[17,18] The collapse of cavitation bubbles results in the generation of extreme temperatures and pressures.[19−21] These local effects produce a variety of radicals and highly active intermediates, which may then initiate or induce material modifications. In recent years, new applications and the effect of ultrasound on mechanical, physical, or chemical changes of materials have received broad attention, especially in catalyst preparation. Kumar et al. synthesized the Pt modified ZSM-5 and β-zeolite catalysts under UIr.[19] Tangestaninejad prepared vanadium polyoxometalate supported MSM-41 under UIr.[20] However, few attempts have been made to investigate the effects of ultrasound on the preparation of metal ion-loaded AC and its influence on the adsorption of DBT on such prepared adsorbents.

The objective of this work is to study the adsorption of DBT on metal ion-supported ACs prepared by UI. Three transition metal ions (Cu(II), Ag(I), and Fe(III)) were separately impregnated on the ACs prepared both in the presence and in the absence of UIr. The adsorption isotherms of DBT on the ion-impregnated ACs were measured with a static adsorption method. The prepared ACs were characterized by nitrogen adsorption experiments, X-ray photoelectron spectroscopy (XPS), and CO-chemisorption. The effects of UIr on the surface area, metallic dispersion, and average particle size loaded on the ACs and its adsorption of DBT are discussed and reported here.

2. Experimental Section

2.1. Materials. The adsorbate, DVT (98 %), was purchased from Acros Organics (NJ, USA). The AC [(40 to 60) mesh] based on coconut shell was supplied by the Zhaoyang Senyuan Activated Carbon Company (China). $AgNO_3$, $Cu(NO_3)_2$, $Fe(NO_3)_3$, and *n*-octane were all analytical reagents.

2.2. Adsorbent Preparation. Adsorbents Ag/AC-UI, Cu/AC-UI, and Fe/AC-UI were separately prepared by impregnating ACs with corresponding metal nitrates under UIr. First, the substrate AC was fully dried by degassing in vacuum at 393 K for 12 h. After degassing, 10 g of ACs were mixed with 100 mL of metal nitrate $AgNO_3$, $Cu(NO_3)_2$, and $Fe(NO_3)_3$ in an aqueous solution (0.01 M), separately, with the pH value kept at around 5. The mixtures were stirred for 0.5 h at room temperature. After that, the three AC−metal nitrate mixtures were set under the treatment of UIr (ultrasonic cleaner KQ-500 VDE, Zhangjiang Kunshan Ultrasonic Electronic Co. Ltd., China). Then, the mixtures were further stirred for 24 h at room temperature. Finally, the slurries were dried at 393 K overnight to remove the solvent and the moisture completely, and then the samples were kept in an airtight bottle for use.

To select proper ultrasonic conditions for adsorbent preparation, different amounts of ultrasonic power [(30, 40, and 50) W], ultrasonic frequency [(28, 45, and 100) kHz], and operating time [(15, 30, 45, and 60) min] were applied on Cu/AC preparation. The optimal conditions were selected based on the adsorption capacity of DBT over the prepared Cu/AC-UI.

For comparison, adsorbents Ag/AC, Cu/AC, and Fe/AC were prepared by impregnation without UIr.

2.3. Model Sulfur Solutions. In the present study, a model sulfur solution was prepared by adding DBT to liquid *n*-octane with the concentration of 0.01 mol·L^{-1} (376 ppmw).

2.4. Adsorption Experiments. Adsorption experiments were conducted in a stirred batch system using a temperature-controlled shaker. The adsorbents [(0.03 to 1.0) g] were separately added into a series of 10 mL test tubes, each filled with 5 mL of DBT solution with an initial concentration of 0.01 mol·L^{-1}. Then the test tubes were sealed. After that, they were placed in a thermostatic shaker bath and shaken at 100 rpm for 48 h. During the adsorption, the system temperature was kept constant at 303 K.

After the equilibrium, the sulfur concentrations of the treated samples were analyzed by high-performance liquid chromatography (HPLC). The chromatographic separation was achieved on an ODS-C$_{18}$ column at 298 K. The mobile phase composition was 100 % HPLC grade methanol. The flow-rate was 1.0 mL·min^{-1}, and the eluent was monitored at 220 nm through a UV detector.

The equilibrium amount adsorbed q_i of DBT on the adsorbent was determined on the basis of the following material balance equation:

$$q_i = \frac{V}{M_i} \cdot (C_0 - C_i^*) \tag{1}$$

where q_i is the equilibrium adsorption capacity of sulfur on the adsorbent (mg-S·g^{-1}), C_0 and C_i^* are the initial and equilibrium concentration of sulfur solutions (mg-S·L^{-1}), respectively, V is the volume of solution (L), and M_i is the mass of the adsorbent used (g).

2.5. Characterization of Adsorbents. 2.5.1. Nitrogen Adsorption Experiments. The textural features of adsorbents were measured by physical adsorption of N_2 at 77 K using a Micromeritics ASAP2010 surface area and porosimetry analyzer. The Brunauer−Emmett−Teller (BET) surface area was calculated from adsorption isotherms using the standard BET equation. The *t*-plot method was applied to derive the micropore surface area.[22]

2.5.2. X-Ray Photoelectron Spectroscopy (XPS). XPS characterization of Cu/AC and Cu/AC-UI, Ag/AC and Ag/AC-UI, and Fe/AC and Fe/AC-UI was carried out to study the element composition of copper, silver, and iron ions in the metal ion-impregnated ACs prepared in the presence and absence of ultrasound. A spectrometer from Surface Science Instruments SSX 100/206 photoelectron was employed. Spectra were registered after the samples were purged at room temperature under vacuum. The residual pressure in the analysis chamber during the analysis was about 10^{-6} Pa. Flood gun energy was adjusted at 10 eV. Survey spectrum and C1s, O1s, Cu2p, Ag3d, and Fe2p spectra were recorded again to check the stability of charge compensation as a function of time. Data treatment was performed with regard to C−(C, H) component of the C1s peak fixed at 285.0 eV.[23] The atomic ratios were calculated from atomic sensitivity factors provided by the manufacturer.

2.5.3. CO-Chemisorption. CO-chemisorption experiments are usually used to determine metal dispersion, metal surface area, and active metal particle size of catalysts. The amount of CO irreversibly held on the surface of the catalyst was measured by a dynamic method on an Auto Chem 2920 instrument (Micromeritics, USA). Prior to adsorption measurements, the sample was reduced in a flow of 10 % H$_2$/Ar (50 mL·min^{-1}) at 350 °C for 2 h and then flushed with pure helium flow (50 mL·min^{-1}) for 0.5 h at the same temperature. The temperature was then brought to room temperature, and CO pulses were injected over the reduced catalyst. CO adsorption was assumed to be completed after three successive peaks showed the same peak areas. Assuming a stoichiometry of one CO molecule per surface metal atom, the dispersion can be calculated. A CO$_{irr}$/Cu = 1 stoichiometry was consequently taken as a reasonable
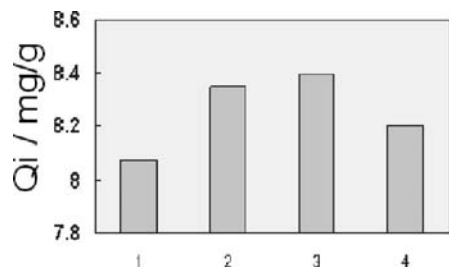
Figure 1. DBT adsorption capacities of the Cu(II)/AC-UI prepared under conditions of different ultrasonic frequency: (1) no ultrasound; (2) 28 kHz; (3) 45 kHz; (4) 100 kHz.

Figure 2. DBT adsorption capacity of the Cu(II)/AC-UI prepared under condition of different ultrasonic intensity: (1) no ultrasound; (2) 30 W; (3) 40 W; (4) 50 W.

Figure 3. DBT adsorption capacity of the Cu(II)/AC-UI prepared under condition of different irradiation time: (1) no ultrasound; (2) 15 min; (3) 30 min; (4) 45 min; (5) 60 min.

estimate in determining Cu dispersion.[24] The following equations[25] are used in a pulse chemisorption analysis to calculate the Cu dispersion, metal surface area, and active particle size:

$$P_D = 100 \frac{CO_{irr} SF_{calc}}{SW_{22414}} g \quad (2)$$

where P_D is percent dispersion, CO_{irr} is the amount of CO irreversibly held on the surface of the catalyst (cm³ at STP), SF_{calc} is the calculated stoichiometry factor, SW is metal content (g), and g is gram molecular weight (g·g⁻¹·mol⁻¹).

The metal surface area ($SA_{Metallic}$, m²·g⁻¹ Cu) was calculated from CO_{irr} uptake using the relationship:

$$SA_{Metallic} = \left(\frac{CO_{irr}}{SW_{22414}}\right) SF_{calc} (6.023 \cdot 10^{23})(SA_{calc}) \quad (3)$$

where $SA_{Metallic}$ is the metallic surface area (m²·g⁻¹ of metal) and SA_{calc} is the calculated specific surface area (per gram of metal), that is, 0.068 nm² for Cu. The Cu crystallite size (d, nm) was calculated from the estimated metal surface area ($SA_{Metallic}$) according to the following equation:

$$d = \frac{6}{\rho SA_{Metallic}} \quad (4)$$

where d is the active particle size (nm) and q is the density of Cu metal, that is, 8.92 g·cm⁻³.

3. Results and Discussion

3.1. Effects of Ultrasonic Radiation Conditions on Adsorption Capacities of Copper-Based ACs for DBT. Figure 1 shows a comparison of DBT adsorption capacities of the Cu(II)/AC-UI prepared under conditions of different ultrasonic frequency. It indicates that the Cu(II)/AC-UI prepared by using an ultrasonic frequency of 45 kHz had the highest adsorption capacity of DBT. Figure 2 gives a comparison of DBT adsorption capacities of the Cu(II)/AC-UI prepared under conditions of different ultrasonic intensity, and it indicates that the Cu(II)/AC-UI prepared by using an ultrasonic intensity of 40 W had the highest adsorption capacity of DBT. Figure 3 gives a comparison of DBT adsorption capacities of the Cu(II)/AC-UI prepared under conditions of different ultrasonic time, and it indicates that the Cu(II)/AC-UI prepared by using an ultrasonic time of 30 min had the highest adsorption capacity of DBT. At the same time, it was also noticed that the application of UIr to prepare the copper ion-impregnated AC improved its adsorption of DBT in comparison to the cases of
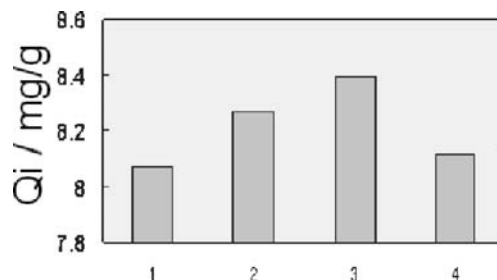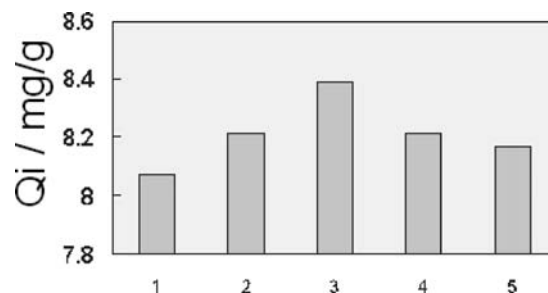
impregnation without UIr. Therefore, the optimal ultrasonic conditions were considered to be an ultrasonic frequency of 45 kHz, ultrasonic power of 40 W, and irradiation time of 30 min. These conditions were set as the standard conditions in this study.

3.2. Isotherms of DBT on the ACs Modified in the Presence and Absence of UIr. Figure 4 shows the isotherms of DBT on the ACs modified in the presence and absence of UIr. It can be seen that the loading of different transition metal ions on the AC surfaces resulted in the variation of DBT adsorption capacity of the modified ACs. For three ACs modified in the presence of UIr, the equilibrium adsorption capacity of DBT over these ACs studied followed the order of Ag/AC-UI > Cu/AC-UI > AC > Fe/AC-UI. In comparison with the original AC, the adsorption performance of the Ag/AC-UI and Cu/AC-UI for DBT improved, while that of the Fe/AC-UI became poor. At the same time, for three ACs modified in the absence of UIr, the same order, Ag/AC > Cu/AC > AC > Fe/AC, was observed, which would be interpreted by means of the HSAB principles[20] later. In addition, it was found that the adsorption capacity of the Ag/AC-UI and Cu/AC-UI for DBT was higher than that of the Ag/AC and Cu/AC, respectively. However, the adsorption capacity of the Fe/AC-UI for DBT was somewhat lower than that of the Fe/AC. That is to say, impregnation under UIr changed the ACs' adsorption performance of DBT, which will be further explained by characterization results of the ACs.

In this work, the hard and soft acid and base (HSAB) principle[26] proposed by Pearson is applied to explain the effects of the local hardness of the carbon surfaces, varied by loading Ag, Cu, and Fe metal ions on its adsorption of DBT. Generally speaking, the adsorption properties of an adsorbent are not only determined by their porous microtexture but are also strongly influenced by the chemical property of their surface. When metal ions with different hardness were separately loaded onto the ACs, the local hardness of the AC surfaces would vary and thus affected the interaction of the AC surfaces with an
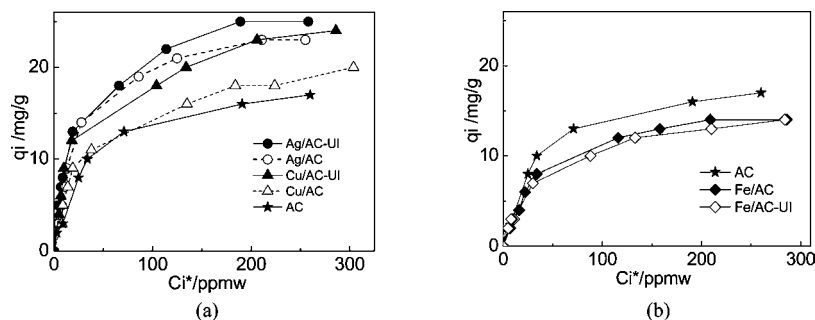
Figure 4. Isotherms of DBT at 30 °C on adsorbents (a) Ag/AC, Ag/AC-UI, Cu/AC, Cu/AC-UI, and AC; (b) AC, Fe/AC, and Fe/AC-UI.

Table 1. Pearson Classification and Absolute Hardness of Metal Ions[24]

metal ions	Ag(I)	Cu(II)	Fe(III)
Pearson classification	soft acid	borderline	hard acid
absolute hardness, η	6.9	8.3	13.1

Table 2. Textural Properties of ACs

adsorbent	AC	Ag/AC	Cu/AC	Fe/AC
BET surface area/$m^2 \cdot g^{-1}$	1187	1036	1110	1077
micropore area/$m^2 \cdot g^{-1}$	718	522	516	558
		Ag/AC-UI	Cu/AC-UI	Fe/AC-UI
BET surface area/$m^2 \cdot g^{-1}$		1071	1178	1080
micropore area/$m^2 \cdot g^{-1}$		599	619	570

adsorbate. In this case, the HSAB principle was locally applied as "hard regions of a system prefer to interact with hard reagents, whereas soft regions prefer soft species".[27]

To make a quantitative calculation of the hardness, density functional theory (DFT) was used by Parr and Pearson.[28] According to this theory, the absolute hardness and electronegativity of DBT can be estimated using the following formula[28,29] to quantitatively confirm its soft/hard property.

$$\eta = 1/2(I - A) \tag{5}$$

where η, the absolute hardness (always positive), is half the difference between I, the ionization energy, and A, the electron affinity. I and A can be calculated using the following equations:

$$I = -E_{HOMO} \tag{6}$$

$$A = -E_{LUMO} \tag{7}$$

Inserting eqs 6 and 7 into eq 5, one can get

$$\eta = -1/2(E_{HOMO} - E_{LUMO}) \tag{8}$$

and

$$\chi = 1/2(I + A) = -1/2(E_{HOMO} + E_{LUMO}) \tag{9}$$

where E_{LUMO} is the lowest unoccupied molecular orbital (LUMO) energy; E_{HOMO} is the highest occupied molecular orbital (HOMO) energy; χ is the electronegativity.

In this work, Hyperchem 7.0 program systems were used to calculate the charge distribution, E_{LUMO} and E_{HOMO} of the DBT molecules. The basis set was 3-21G. Then the absolute hardness η and electronegativity of DBT were calculated as 5.267 and 2.673. In terms of Pearson hard−soft base classification, DBT was considered as a soft base due to its absolute electronegativity < 2.8.[26,28,29] On the other hand, the transition metal ions were taken as Lewis acids,[30] as indicated in Table 1. According to the Pearson classification, the ion Ag(I) is a soft acid, the ion Cu(II) is a borderline acid, and the ion Fe(III) is a hard acid.

When these different metal ions were separately loaded onto the AC surfaces, the surface local hardness of the ACs would be changed.

For the modified ACs prepared by the impregnation method, according to the HSAB principle that hard acids prefer to bond to hard bases, and soft acids prefer to bond to soft bases,[26,28−30] it can be predicted that the loading of Ag(I) could enhance the interaction between DBT and Ag/AC surfaces because Ag(I) is a soft acid, while DBT is a soft base. In addition, it can be also predicted that the loading of Fe(III) will most possibly weaken the interaction between DBT and Fe/AC surfaces because Fe(III) is a hard acid. It should also noticed that the equilibrium adsorption capacity of DBT over Cu/AC was also improved compared to the original AC, as shown in Figure 4a, suggesting the loading of this borderline acid ion would enhance the interaction between DBT and the resulting AC surfaces. This is possibly because Cu(II) was the borderline acid; the loading of borderline acidic Cu(II) on the surface of the AC could weaken the local hard acid of the surface, thus enhancing adsorption of DBT to some extent.[31]

Furthermore, it can be seen from Figure 4a that the equilibrium adsorption capacities of DBT over Ag/AC-UI and Cu/AC-UI were respectively higher than those on the corresponding Ag/AC and the Cu/AC prepared in the absence of ultrasound, indicating that the use of ultrasound in the preparation of the Ag/AC-UI and the Cu/AC-UI could improve their adsorption capacity of DBT. This phenomenon was further explained by the following characterization results.

In this work, the prepared Ag/AC-UI showed the highest adsorptive capacity. It showed around 4 times higher DBT capacity than carbon aerogel (CA) monoliths (22 nm CA) at the sulfur equilibrium concentration of 100 ppmw, compared to the DBT isotherms reported by Haji and Erkey.[32] It also shows comparable DBT capacity as several microporous coordination polymers at the sulfur equilibrium concentration in the range of (0 to 300) ppm, compared to the DBT isotherms reported by Cychosz et al.[33]

3.3. Characterization of the Modified ACs. 3.3.1. Textural Properties of the Modified ACs. Table 2 lists the textural features of the modified ACs, including BET surface area and micropore area. It indicates that the BET surface area of the modified ACs was somewhat smaller than that of the original AC, and their micropore area became obviously smaller
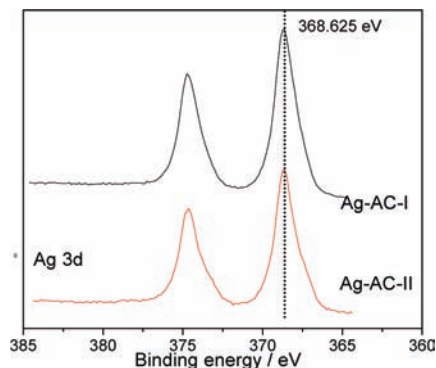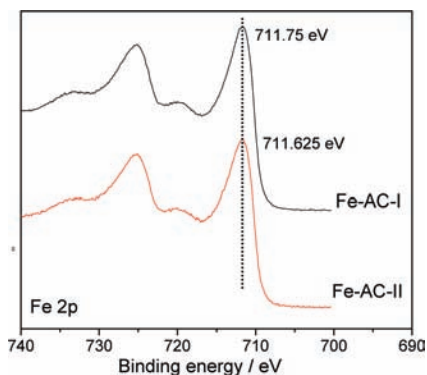
Figure 5. XPS patterns of Ag/AC and Ag/AC-UI.

Figure 6. XPS patterns of Fe/AC and Fe/AC-UI.

Figure 7. XPS patterns of Cu/AC and Cu/AC-UI.

Table 3. Metallic Dispersion (*R*), Surface Area (*S*), and Average Particle Size (*D*) of the Metallic Particles Loaded on the ACs

	R	*S*	*D*
	%	$m^2 \cdot g^{-1}$	nm
Ag/AC	4.37	21.22	26.92
Ag/AC-UI	8.53	41.41	13.80
Cu/AC	6.89	44.43	15.14
Cu/AC-UI	15.62	100.70	6.68
Fe/AC	2.34	15.48	49.19
Fe/AC-UI	4.19	27.71	27.47

compared to the original AC. On the other hand, it was noticed that the BET surface area of these modified ACs was very close. However, their micropore area was slightly different. The ACs modified in the presence of UI, Ag/AC-UI, Cu/AC-UI, and Fe/AC-UI had a somewhat higher micropore area in comparison with those ACs modified in the absence of UI, which may possibly be ascribed to the finer metallic particle size and better dispersion on the surfaces of the ACs modified in the presence of UI.

3.3.2. XPS Spectra of the Modified ACs. XPS was conducted to obtain information on the elemental composition and oxidation state. Figures 5 to 7 show the XPS spectra of the modified ACs, such as Cu/AC, Cu/AC-UI, Ag/AC, Ag/AC-UI, Fe/AC, and Fe/AC-UI. Figure 5 shows that the peaks of the silver core line $3d_{5/2}$ at 368.625 eV[34,35] on both the Ag/AC and the Ag/AC-UI were typical of Ag(I) species, suggesting that elemental silver has been effectively loaded on the carbon surfaces in the presence of Ag(I). Figure 6 shows that the binding energies of Fe $2p_{3/2}$[35] were separately at 711.75 eV on Fe/AC and 711.625 eV on Fe/AC-UI, suggesting that elemental iron has been effectively loaded on the carbon surfaces. Figure 7 clearly shows that there are shakeup satellite peaks[36,37] at (942.7 and 961.2) eV in the XPS spectra of the Cu/AC and Cu/AC-II, which were usually characteristic of Cu(II) species, suggesting that elemental copper has been effectively loaded on the carbon surfaces.

3.3.3. CO-Chemisorption of the Modified ACs. Table 3 shows the physical properties of the metal components loaded on ACs studied, such as dispersion, metal surface area, and average particle size of metallic crystal−components over the surfaces of the ACs, which were calculated from CO irreversible adsorption.

The data in Table 3 indicated that, for a pair of Ag/AC-UI and Ag/AC, Cu/AC-UI and Cu/AC, or Fe/AC-UI and Fe/AC, the average particle size of the metallic component loaded on the ACs prepared in th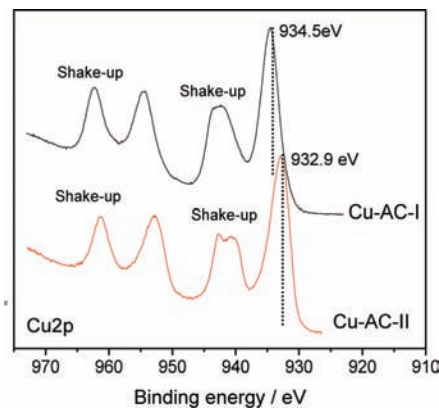e presence of ultrasound was much smaller than that prepared in the absence of ultrasound, and more importantly, both dispersion (*R* %) and surface area per gram of metal on the Ag/AC-UI, Cu/AC-UI, and Fe/AC-UI were respectively higher than those on the corresponding ACs such as Ag/AC, Cu/AC, and Fe/AC. This suggests that the use of UIr in the modification of ACs can make metallic particles become finer and obtain a good dispersion on the carbon surfaces in comparison to the case of only using impregnation. It is the difference in the dispersion (*R* %) and surface area per gram of metal on the carbon surfaces that results in the variation of the DBT adsorption capacities of the modified ACs. Moreover, positive or negative effects of better dispersed metals on DBT adsorption depend on the property of different metals as discussed earlier in Table 1. For the pair of the Ag/AC-UI and Ag/AC, the Ag/AC-UI has higher dispersion (*R* %) and surface area per gram of Ag on its surfaces, and thus its DBT adsorption capacity becomes greater since the loading of Ag has a positive role in improvement of DBT adsorption. Similarly, for the pair of the Cu/AC-UI and Cu/AC, since the loading of Cu has a positive role in improvement of DBT adsorption as stated above, the Cu/AC-UI has a higher DBT adsorption capacity due to its having higher dispersion (*R* %) and surface area per gram of Cu on its surfaces, However, for the pair of the Fe/AC-UI and Fe/AC, since the loading of Fe could weaken the interaction DBT with carbon surfaces, the Fe/AC-UI has a slightly lower DBT adsorption capacity due to its higher dispersion (*R* %) and surface area per gram of Fe on its surfaces in comparison with the Fe/AC.

4. Conclusion

From ongoing discussion, the following conclusions can be drawn:

(1) The use of different metal salt solutions to impregnate the ACs can change their adsorption abilities toward DBT. The loading of Ag^+ on the AC improved the adsorption capacity of Ag(I)/AC surfaces toward DBT because Ag^+ is a soft acid and DBT is a soft base, whereas the loading of Fe^{3+} weakened the adsorption capacity of the Fe(III)/AC surfaces toward DBT

because Fe^{3+} is a hard acid. The amount adsorbed of DBT on the modified ACs follows the order: Ag/AC > Cu/AC > AC > Fe/AC.

(2) The modification methods have obviously influenced the adsorption abilities of the modified ACs toward DBT. The application of UIr to prepare metal ion-impregnated ACs can make metallic particles become finer and get better dispersion on the carbon surfaces in comparison with the use of impregnation only. As a consequence, the Ag/AC-UI and Cu/AC-UI prepared by using the UI have higher adsorption capacities of DBT respective to the Ag/AC and Cu/AC prepared using impregnation.

Literature Cited

(1) Kim, J. H.; Ma, X.; Zhou, A.; Song, C. Ultra-deep desulfurization and denitrogenation of diesel fuel by selective adsorption over three different adsorbents: A study on adsorptive selectivity and mechanism. *Catal. Today* **2006**, *111*, 74–83.

(2) Song, C. An overview of new approaches to deep desulfurization for ultra-clean gasoline, diesel fuel and jet fuel. *Catal. Today* **2003**, *86*, 211–263.

(3) Belliere, V.; Lorentz, C.; Geantet, C.; Yoshimura, Y.; Laurenti, D.; Vrinat, M. Kinetics and mechanism of liquid-phase alkylation of 3-methylthiophene with 2-methyl-2-butene over a solid phosphoric acid. *Appl. Catal., B* **2006**, *64*, 254–261.

(4) Babich, I. V.; Moulijn, J. A. Science and technology of novel processes for deep desulfurization of oil refinery stream: a review. *Fuel* **2003**, *82*, 607–631.

(5) Cristol, S.; Paul, J. F.; Payen, E.; Bougeard, D.; Hutschka, F.; Clémendot, S. DBT derivatives adsorption over molybdenum sulfide catalysts: a theoretical study. *J. Catal.* **2004**, *224*, 138–147.

(6) Gonzalez-Olmos, R.; Iglesias, M. Thermodynamics and kinetics of fuel oxygenate adsorption into granular activated carbons. *J. Chem. Eng. Data* **2008**, *53*, 2556–2561.

(7) EI-Sharkawy, I. I.; Ming, H. J.; Ng, K. C.; Yap, C.; Saha, B. B. Adsorption equilibrium and kinetics of gasoline vapors onto carbon-based adsorbents. *J. Chem. Eng. Data* **2008**, *53*, 41–47.

(8) Ming, H. J.; Ng, K. C.; Yap, C.; Saha, B. B. Effect of pressure on the adsorption rate for gasoline vapor on pitch-based activated carbon. *J. Chem. Eng. Data* **2009**, *54*, 1504–1509.

(9) Borkar, C.; Tomar, D.; Gumma, S. Adsorption of dichloromethane on activated carbon. *J. Chem. Eng. Data* **2010**, *55*, 1640–1644.

(10) Liu, F.; Wang, J.; Li, L.; Shao, Y.; Xu, Z.; Zheng, S. Adsorption of direct yellow 12 onto ordered mesoporous carbon and activated carbon. *J. Chem. Eng. Data* **2009**, *54*, 3043–3050.

(11) Wang, Y.; Yang, R. T. Desulfurization of Liquid Fuels by Adsorption on Carbon-Based Sorbents and Ultrasound-Assisted Sorbent Regeneration. *Langmuir* **2007**, *23*, 3825–3831.

(12) Ania, C. O.; Bandosz, T. J. Metal-loaded polystyrene-based activated carbons as dibenzothiophene removal media via reactive adsorption. *Carbon* **2006**, *44*, 2404–2412.

(13) Zhou, A.; Ma, X.; Song, C. Liquid-Phase Adsorption of Multi-Ring Thiophenic Sulfur Compounds on Carbon Materials with Different Surface Properties. *J. Phys. Chem. B* **2006**, *110*, 4699–4707.

(14) Zhou, A.; Ma, X.; Song, C. Effects of oxidative modification of carbon surface on the adsorption of sulfur compounds in diesel fuel. *Appl. Catal., B* **2009**, *87*, 190–199.

(15) Yu, M.; Li, Z.; Ji, Q.; Wang, S.; Su, D.; Lin, Y. S. Effect of thermal oxidation of activated carbon surface on its adsorption towards Dibenzothiophene. *Chem. Eng. J.* **2009**, *48*, 242–247.

(16) Zhu, L.; Zhang, H. A novel method for the modification of zinc powder by ultrasonic impregnation in cerium nitrate solution. *Ultrason. Sonochem.* **2008**, *15*, 393–401.

(17) Hamdaoui, O.; Djeribi, R.; Naffrechoux, E. Desorption of Metal Ions from Activated Carbon in the Presence of Ultrasound. *Ind. Eng. Chem. Res.* **2005**, *44*, 4737–4744.

(18) Susiiik, K. S.; Choet, S. B.; Cichowlas, A. A.; Grinstaff, M. W. Sonochemical synthesis of amorphous iron. *Nature* **1991**, *353*, 414–416.

(19) Kumar, N.; Masloboischikova, O. V.; Kustov, L. M.; Heikkila, T.; Salmi, T.; Murzin, D. Y. Synthesis of Pt modified ZSM-5 and beta zeolite catalysts: Influence of ultrasonic irradiation and preparation methods on physicochemical and catalytic properties in pentane isomerization. *Ultrason. Sonochem.* **2007**, *14*, 122–130.

(20) Tangestaninejad, S.; Mirkhani, V.; Moghadam, M.; Mohammadpoor-Baltork, I.; Shams, E.; Salavati, H. Hydrocarbon oxidation catalyzed by vanadium polyoxometalate supported on mesoporous MCM-41 under ultrasonic irradiation. *Ultrason. Sonochem.* **2008**, *15*, 438–447.

(21) He, Z.; Traina, S. J.; Bigham, J. M.; Weavers, L. K. Sonolytic Desorption of Mercury from Aluminum Oxide. *Environ. Sci. Technol.* **2005**, *39*, 1037–1044.

(22) Wu, Y.; Li, Z.; Xi, H. Influence of the microporosity and surface chemistry of polymeric resins on adsorptive properties toward phenol. *J. Hazard. Mater.* **2004**, *113*, 131–135.

(23) Fu, X.; Yu, H.; Peng, F.; Wang, H.; Qian, Y. Facile preparation of RuO_2/CNT catalyst by a homogenous oxidation precipitation method and its catalytic performance. *Appl. Catal., A* **2007**, *321*, 190–197.

(24) Pan, H.; Xu, M.; Li, Z.; Huang, S.; He, C. Catalytic combustion of styrene over copper based catalyst: Inhibitory effect of water vapor. *Chemosphere* **2009**, *76*, 721–726.

(25) Chary, K. V. R.; Naresh, D.; Vishwanathan, V.; Sadakane, M.; Ueda, W. Vapor phase hydrogenation of phenol over Pd/C catalysts: a relationship between dispersion, metal area and hydrogenation activity. *Catal. Commun.* **2007**, *8*, 471–477.

(26) Pearson, R. G. Hard and soft acids and bases. *J. Am. Chem. Soc.* **1963**, *85*, 3533–3539.

(27) Lee, C.; Wang, Y.; Parr, R. G. *J. Mol. Struct.: THEOCHEM* **1988**, *163*, 305.

(28) Parr, R. G.; Pearson, R. G. Absolute hardness: companion parameter to absolute electronegativity. *J. Am. Chem. Soc.* **1983**, *105*, 7512–7516.

(29) Pearson, R. G. The HSAB principle - more quantitative aspects. *Inorg. Chim. Acta* **1995**, *240*, 93–98.

(30) Xiao, J.; Li, Z.; Liu, B.; Xia, Q.; Yu, M. Adsorption of benzothiophene and dibenzothiophene on ion-impregnated activated carbons and ion-exchanged Y zeolites. *Energy Fuels* **2008**, *22*, 3858–3863.

(31) Putz, M. V.; Russo, N.; Siclia, E. On the applicability of the HSAB principle through the use of improved computational schemes for chemical hardness evaluation. *J. Comput. Chem.* **2004**, *25*, 994–1003.

(32) Haji, S.; Erkey, C. Removal of Dibenzothiophene from Model Diesel by Adsorption on Carbon Aerogels for Fuel Cell Applications. *Ind. Eng. Chem. Res.* **2003**, *42*, 6933–6937.

(33) Cychosz, K. A.; Wong-Foy, A. G.; Matzger, A. J. Liquid Phase Adsorption by Microporous Coordination Polymers: Removal of Organosulfur Compounds. *J. Am. Chem. Soc.* **2008**, *130*, 6938–6939.

(34) Hadnadjev, M.; Vulic, T.; Marinkovic-Neducin, R.; Suchorski, Y.; Weiss, H. The iron oxidation state in Mg-Al-Fe mixed oxides derived from layered double hydroxides: An XPS study. *Appl. Surf. Sci.* **2008**, *254*, 4297–4302.

(35) Lamouroux, E.; Serp, P.; Kihn, Y.; Kalck, P. Identification of key parameters for the selective growth of single or double wall carbon nanotubes on FeMo/Al_2O_3 CVD catalysts. *Appl. Catal., A* **2007**, *323*, 162–173.

(36) Dai, W.; Sun, Q.; Deng, J.; Wu, D.; Sun, Y. XPS studies of Cu/ZnO/Al_2O_3 ultra-fine catalysts derived by a novel gel oxalate co-precipitation for methanol synthesis by CO_2 + H_2. *Appl. Surf. Sci.* **2001**, *177*, 172–179.

(37) Agrell, J.; Birgersson, H.; Boutonnet, M.; Melián-Cabrera, I.; Navarro, R. M.; Fierro, J. L. G. Production of hydrogen from methanol over Cu/ZnO catalysts promoted by ZrO_2 and Al_2O_3. *J. Catal.* **2003**, *219*, 389–403.